HHS Public Access

Author manuscript

Biochim Biophys Acta Mol Basis Dis. Author manuscript; available in PMC 2022 February 04.

Published in final edited form as:

Biochim Biophys Acta Mol Basis Dis. 2021 October 01; 1867(10): 166179. doi:10.1016/j.bbadis.2021.166179.

Mice with Dysfunctional TGF-β Signaling Develop Altered Intestinal Microbiome and Colorectal Cancer Resistant to 5FU

Zhuanhuai Wang[a], **Lindsay M. Hopson**[b], **Stephanie S. Singleton**[b], **Xiaochun Yang**[a], **Wilma Jogunoori**[c], **Raja Mazumder**[b], **Vincent Obias**[d], **Paul Lin**[d], **Bao-Ngoc Nguyen**[a], **Michael Yao**[e], **Larry Miller**[f], **Jon White**[d], **Shuyun Rao**[a,*], **Lopa Mishra**[a,f,g,*]

[a]Center for Translational Medicine, Department of Surgery, The George Washington University, Washington, DC, USA

[b]Department of Biochemistry and Molecular Medicine, The George Washington University, Washington, DC, USA

[c]Research and Development, Veterans Affairs Medical Center, Washington, DC, USA

[d]Department of Surgery, The George Washington University, Washington, DC, USA.

[e]Department of Gastroenterology, Veterans Affairs Medical Center, Washington, DC, USA

[f]Divisions of Gastroenterology and Hepatology, Northwell Health, New Hyde Park, Long Island, NY, USA.

[g]The Institute for Bioelectronic Medicine, Feinstein Institutes for Medical Research and Cold Spring Harbor Laboratory.

Abstract

Emerging data show a rise in colorectal cancer (CRC) incidence in young men and women that is often chemoresistant. One potential risk factor is an alteration in the microbiome. Here, we investigated the role of TGF-β signaling on the intestinal microbiome and the efficacy of chemotherapy for CRC induced by azoxymethane and dextran sodium sulfate in mice. We used two genotypes of TGF-β-signaling-deficient mice (*Smad4*$^{+/-}$ and *Smad4*$^{+/-}$/*Sptbn1*$^{+/-}$), which developed CRC with similar phenotypes and had similar alterations in the intestinal microbiome. Using these mice, we evaluated the intestinal microbiome and determined the effect of dysfunctional TGF-β signaling on the response to the chemotherapeutic agent 5-Fluoro-uracil (5FU) after induction of CRC. Using shotgun metagenomic sequencing, we determined gut microbiota composition in mice with CRC and found reduced amounts of beneficial species of *Bacteroides* and *Parabacteroides* in the mutants compared to the WT mice. Furthermore, the

[*]**Correspondence:** Lopa Mishra, M.D., Professor of Medicine, Merinoff Endowed Chair, and Co-Director, The Institute for Bioelectronic Medicine, Feinstein Institutes for Medical Research and Cold Spring Harbor Laboratory, Attending Physician, Divisions of Gastroenterology and Hepatology, Northwell Health, 350 Community Drive, Manhasset, NY 11030, Tel: 240-401-2916, lopamishra2@gmail.com, lmishra1@northwell.edu, Shuyun Rao, PhD, Assistant Professor, Center for Translational Medicine, George Washington University, 2300 Eye Street, NW Ross Hall 554, Washington DC, 20037, Tel: 202-994-4629, raoshuyun@gwu.edu.

CrediT Author contributions

ZW-data analyses, in vivo experiments, manuscript preparation; SS, LH, RM, SR-microbiome data analyses; XY- in vivo experiments; LM, SR- supervised the study with input from VO, PL, BNN, MY, LM, and JW.

Declaration of competing interest: The authors declare that they have no known competing financial interests or personal relationships that could have appeared to influence the work reported in this paper.

mutant mice with CRC were resistant to 5FU. Whereas the abundances of *E. boltae*, *B.dorei*, *Lachnoclostridium sp.*, and *Mordavella sp.* were significantly reduced in mice with CRC, these species only recovered to basal amounts after 5FU treatment in WT mice, suggesting that the alterations in the intestinal microbiome resulting from compromised TGF-β signaling impaired the response to 5FU. These findings could have implications for inhibiting the TGF-β pathway in the treatment of CRC or other cancers.

Keywords

chemoresistance; microbiome; colorectal cancer; TGF-β signaling; Bacteroides; 5FU

1. Introduction

Advanced colorectal cancer (CRC) is the third most commonly diagnosed cancer in the world and remains both lethal and difficult to treat, with over 130,000 new cases per year in the U.S. [1]. Several critical drivers and pathways important for the initiation and progression of CRC have been characterized [2–8]. These include the TGF-β, WNT, RAS-MAPK, PI3K, P53, and DNA mismatch-repair pathways [9, 10].

The TGF- β pathway is commonly altered in many human cancers. The Cancer Genome Atlas (TCGA) studies show that mutations affecting TGF-β signaling are observed in >80% of proximal colon carcinomas [11]. Depending on the context, this pathway can be tumor suppressive (typically early in tumorigenesis) or can promote metastasis (typically late in cancer progression) [12–15]. TGF-β is a key regulator of multiple biological processes, including cell proliferation, differentiation, migration, and apoptosis, and multiple types of cells, including epithelial cells, immune cells, fibroblasts, and cancer cells [16–20]. Ligands of the TGF-β subfamily bind and activate the serine-threonine kinase type II TGF- β receptors (TGFBR2), which in turn phosphorylates TGFBR1 and forms an activated ligand-receptor complex. Activated TGFBR1 recruits and phosphorylates downstream receptor-regulated Smad2 and Smad3 at their C-terminal serines, enabling complex formation with SMAD4 [4, 19]. The resulting Smad complex translocates into the nucleus and interacts with other transcription factors in a cell-specific manner to regulate TGF-β–responsive gene expression. The outcome of such Smad activity depends upon multiple factors that include adaptors, such as SARA and SPTBN1, as well as E3 ligases [20]. Downstream targets of TGF-β signaling include genes encoding cell-cycle regulatory proteins that mediate cell cycle arrest [21]. Activated TGF-β also activates Smad-independent activities, including those implicated in CRC, such as MAPK and PI3K signaling [22].

TGF-β signaling functions as a tumor suppressor in normal and premalignant epithelial cells through cell-autonomous roles. Tumor-suppressive functions also involve the stromal tissue through suppression of inflammation and inhibition of stromal-derived mitogens. Current data support TGF-β signaling as a suppressor of colorectal cancers at the early stages [3, 23]. In later diseases, metastatic CRCs escape the tumor-suppressor effects of TGF-β signaling by becoming resistant to TGF-β-induced growth inhibition [24]. Because many

cells and tissues beyond those of the cancerous cells respond to or produce TGF-β, TGF-β signaling may have additional effects in promoting cancer progression [25, 26].

TGF-β signaling is critically important for regulating the gastrointestinal immune system, which in turn influences the gastrointestinal microbial populations [27, 28]. Gastrointestinal (GI) microorganisms can impede chemotherapeutic outcomes by inactivating chemotherapy drugs. In addition, the TGF-β pathway function in concert with microbial signaling in humans [20, 29]. We showed that mice that are genetically deficient in TGF-β-signaling (*Smad4*+/−*Sptbn1*+/−) spontaneously develop CRC when housed under standard conditions [14]. However, *Tgfb1*−/− *Rag2*−/− mice, which are both immune-compromised and unable to respond to TGF-β subfamily ligands, do not develop CRC when housed in a germ-free environment [30]. We observed that altered bacterial composition was associated with colon tumors in the *Smad4*+/−*Sptbn1*+/− mice with defective TGF-β signaling: Some bacterial species, such as *Clostridium septicum,* were increased and other species, such as the beneficial *Bacteroides vulgatus* and *Parabacteroides distasonis*, were decreased [10]. Thus, *Smad4*+/−*Sptbn1*+/− mice represent useful models for assessing the role of TGF-β signaling in CRC and for investigating the role of the microbiota in this process and the response to therapy.

Because studies have linked CRC onset and progression, as well as treatment response, with the gut microbiome [31–33], we investigated the connection between these events and TGF-β signaling using *Smad4*+/− and *Smad4*+/−*Sptbn1*+/− mice to represent TGF-β signaling-defective models. We selected mice heterozygous for *Smad4* because (i) according to data in cBioPortal, more than 63% of human CRCs are heterozygous for the gene encoding a mediator common to TGF-β pathways, *SMAD4* [34], (ii) inactivating mutations in *SMAD4* correlate with metastasis of CRC [35], (iii) reduced abundance of *SMAD4* is associated with poor prognosis in patients receiving 5-fluorouracil (5FU) chemotherapy [36, 37] and (iv) 5FU resistance in an orthotopic mouse model [35].

We hypothesized that defective TGF-β signaling would impact the gut microbiome to produce a signature that correlates with CRC chemotherapy response. We used a well-established model of chemically-induced CRC [38–40] and studied the microbiomes and responses to chemotherapy with 5FU in both WT mice and mice that were TGF-β signaling-deficient (*Smad4*+/− and *Smad4*+/−*Sptbn1*+/−). Our study identified specific changes in the gut microbiome that are associated with 5FU resistance in these mice and showed that the gut microbiome response to 5FU differed between wild-type (WT) and the TGF-β signaling-deficient mice.

2. Materials and Methods

2.1. Generation of transgenic mice

Smad4+/− and *Sptbn1*+/− mutant mice were generated as previously described [10, 14]. *Sptbn1*+/– mice were intercrossed with *Smad4*+/– mice to generate *Smad4*+/–*Sptbn1*+/– mice. Genotypes were confirmed by PCR. All mice were on a 129SvEv/Black Swiss x C57BL/6 background. Both male and female mice from WT mice (n = 16) and TGF-β signaling-deficient mice (*Smad4*+/−/*Sptbn1*+/– mice, n = 12; and *Smad4*+/− mice, n = 6)

between 10 – 16 weeks old were used. Experiments were performed in the conventional unit of the animal facilities at George Washington University Institutional Animal Research Center. All the animal research was approved by The George Washington University Institutional Animal Care and Use Committee.

2.2. Induction of colon cancer

The induction of colitis-associated CRC was performed as previously described [38]. Male and female mice were included in this study. In brief, mice were subjected to intraperitoneal injection (i.p.) with 12.5 mg/kg azoxymethane (AOM; Sigma-Aldrich, A5486, MO, USA) on Day 0. Dextran sodium sulfate (DSS) exposure was initiated at a concentration of 2.5% in drinking water on Day 5 and was administered for five days [39, 40]. DSS cycles were repeated twice with an interval of 14 days of normal drinking water between each cycle. All DSS preparations were renewed after two days. After the third DSS cycle, mice of each genotype were randomly divided into 5FU recipients or phosphate-buffered saline (PBS) controls. Mice were injected (i.p.) with 100 mg/kg 5FU (Sigma-Aldrich, F6627, MO, USA) [41–43] or PBS once a week for four weeks. Seven days after 5FU or PBS treatment, mice were sacrificed, the colon was removed, and macroscopically visible tumors were counted. Assessment of histopathological scores was performed on formalin-fixed, paraffin-embedded (FFPE) colon sections after staining with hematoxylin and eosin (H&E).

2.3. Immunohistochemistry

Cryosections of paraformaldehyde (PFA)-fixed tissue samples were probed with antibodies against Ki67 (Thermofisher Scientific, MA5–14520, IL, USA) and cleaved caspase-3 (Cell signaling, #9664, Danvers, MA 01923). Biotinylated secondary antibodies (Vectastain Elite ABC kit Peroxidase, PK6106, CO, USA), and the DAB kit (Dako, EnVision Dual-link System HRT, K4065, CA, USA) were used for signal amplification and detection. To detect cleaved caspase 3, we used a 1:500 antibody dilution and citrate buffer antigen retrieval. Images were acquired with an Eclipse E800 microscope equipped with a Dxm1200F camera. To quantify cells positive for Ki67 or cleaved caspase 3, cells were counted using the 40× objective by researchers blinded to the treatment condition. Positively stained cells were counted from 5 randomly selected fields on each slide. For Ki67 quantification, the percentage of cells Ki67-positive cells out of the total number of epithelial cells in the field was determined. For caspase 3 quantification, the percentage of positive cells out of the total number of cells in the field was determined.

2.4. Fecal sample collection

Microbial DNA was collected from fecal samples from age-matched and gender-matched WT mice and TGF-β signaling-deficient mice (*Smad4*+/− and *Smad4*+/–/*Sptbn1*+/–). Samples were collected before CRC development and after treatment of CRC. Samples collected before CRC induction were considered “basal” and those after CRC induction and treatment with either 5FU or PBS as CRC (tumor). Mice were generally housed in cages with 5 mice/cage. When collecting fecal samples, mice were temporarily housed in a single autoclaved cage to avoid cross-contamination (2 – 4 fecal pellets per mouse). For microbiome data analyses, we grouped the mice as follows: Before CRC induction as WT basal (n = 16), TGF-β signaling-deficient mice basal [n = 16; *Smad4*+/–/*Sptbn1*+/– (n = 12)

and *Smad4*+/− mice (n = 4)], and after CRC induction as WT-5FU (n = 7), WT-PBS (n = 7), TGF-β signaling-deficient mice PBS [n = 8; *Smad4*+/–/*Sptbn1*+/– (n = 5) and *Smad4*+/− mice (n = 3)], and TGF-β signaling-deficient mice 5FU [n = 10; *Smad4*+/–/*Sptbn1*+/– (n = 7) and *Smad4*+/− mice (n = 3)].

2.5. Shotgun metagenomic sequencing

DNA was extracted from the fecal samples using the QIAmp PowerFecal DNA Extraction Kit (Qiagen, 12830–50, MD, USA). Double-stranded DNA (dsDNA) concentration was assessed by NanoDrop, and the quality was evaluated by the Qubit dsDNA Broad Range DNA Assay Kit26. Samples were prepared for Illumina sequencing following the manufacturer's protocol using the Nextera XT DNA Library Preparation Kit (Illumina, FC-131–1096). Paired-end sequencing was performed using a Mid Output v 2.5 (300 cycles) kit (Illumina, 20024905) on a NextSeq 500, with dual indexing. Each dsDNA molecule was sequenced 150 bases from the end of each strand. Each strand also had an 8-basepair molecular barcode that was sequenced.

2.6. Bioinformatic analysis

The FASTQ files from the shotgun metagenomic sequencing in the previous step were uploaded into the High-Performance Integrated Virtual Environment (HIVE-2) [44] for bioinformatics analysis. The quality of the reads was assessed using quality assurance (QA) and quality check (QC) methods as previously described [45]. Host DNA was removed from all samples prior to metagenomics analysis using HIVE-Hexagon [46] and a representative mouse reference genome, whereby (a) sample reads were aligned to the most representative mouse reference genome, (b) the unaligned reads were archived, and (c) further analysis was conducted on the archived unaligned reads (compiled of microbial DNA). The most representative mouse genome was created by combining a mouse genome (GCA_000001635.26) with mitochondrial mouse DNA with the accessions obtained from proteome UP000000589 [47] using the HIVE tool called Hive-Seq [44]. The following two-step metagenomics analysis pipeline was used to compile the relative abundance dataset [45]. First, the taxonomic composition of each sample was assessed by using CensuScope [48], a HIVE application that performs taxonomic profiling using a census-based sampling algorithm to map sample reads to a nonredundant nucleotide database, FilteredNTv6.0 [45]. All detected organisms with a match count of fewer than 10 reads were removed. Additional manual QC and curation measures were performed to remove any remaining host DNA identified in the CensuScope csv output files, such as plasmids, scaffolds, or primers that were not detected for removal during the initial HIVE-Hexagon step. The final taxonomic data were aggregated into a single csv file, creating a list of unique organisms derived from all the samples; this file was then used as a reference base in the next step. Second, using HIVE-Hexagon [46], a parallelized sequence aligner for NGS data analysis, the archived unaligned reads from each sample were run against the mouseDB. The output from this step includes a csv file per sample that contains taxomonic information and the number of alignments or 'hits' to the mouseDB. Using the number of hits, bacterial relative abundances were calculated per sample, all csv files were aggregated into a single relative abundance dataset, and this final dataset was used for statistical analyses. For *Fusobacterium* analysis, species with the matched count of fewer than 1 read were removed.

2.7. Statistical analysis

Differences between 2 groups were evaluated using 2-tailed Student's t-tests with GraphPad Prism. For multiple comparisons, 1-way ANOVA with post-hoc Bonferroni's test was used. For contingency table comparison, we used Chi-square and Fisher's exact test. Results are presented as mean ± SEM unless otherwise indicated. For all statistical analyses, $p < 0.05$ was considered statistically significant. After normalization, the relative abundance calculated in each sample was plotted using GraphPad Prism 7.0, and an unpaired *t-test* was used for statistical analysis.

3. Results

3.1 TGF-β signaling-deficient mice have a distinct gut microbiome signature

Using a well-established AOM/DSS method to rapidly induce colitis-associated CRC [9, 38–40, 49, 50], we induced CRC in WT, *Smad4+/−Sptbn1+/−*, and *Smad4+/−* mice. Tumors were induced by AOM/DSS administration in all of the mutant mice but only a subset of the WT mice (Table 1). Following the last DSS cycle, all mice were randomly divided into 5FU or control (PBS) groups and administered 5FU or PBS once a week for 4 weeks (Figure 1A).

To identify the association of microbiota with defective TGF-β signaling, shotgun metagenomic analyses were performed in fecal samples collected from both WT and age-matched mutant mice before CRC induction (basal) and after CRC induction and treatment (5FU or PBS). By analyzing several disease-related bacterial species, we found similar commensal intestinal bacterial populations in *Smad4+/−Sptbn1+/−* and *Smad4+/−* mice without CRC (Figure 1B, 1C, 1D). Therefore, we combined the data from both *Smad4+/−Sptbn1+/−* and *Smad4+/−* mice as the TGF-β signaling–deficient (SKO) group for most analyses. When compared with WT controls in the basal condition without CRC, *Smad4+/−Sptbn1+/−* and *Smad4+/−* mice in the basal condition had significantly reduced abundances of many Bacteroides bacteria, including *B. dorei, B.caccae, B. ovatus, B. thetaiotaomicron, B. fragilis*, and the beneficial bacteria *B. vulgatus* and *Parabacteroides distasonis* were also decreased in samples from *Smad4+/− Sptbn1+/−* mice analyzed alone or in combination with samples from *Smad4*+/− (SKO group) (Figure 1B, 1C). These findings are consistent with our previous results from the analysis of the combined samples from *Smad4+/−Sptbn1+/−* and *Sptbn1*+/− mice [10]. The abundance of pathogenic or disease-associated species, such as *Enterococcus faecalis, Alistipes finefoldii, A. shahii,* and *Halomonas sp.*, were significantly increased in *Smad4+/−Sptbn1+/−* mice or SKO compared to the WT controls (Figure 1C). Thus, TGF-β signaling-deficient mice had a unique gut microbiome signature that could contribute to their increased susceptibility to colitis-induced CRC. We also observed an increased abundance of human CRC-associated bacteria, *Fusobacterium nucleatum*, in these TGF-β signaling–deficient mice (*Smad4+/−Sptbn1+/−*, *Smad4+/−* or SKO) when compared to WT mice (Figure 1D).

3.2 TGF-β signaling-deficient mice are more susceptible to AOM/DSS-induced CRC

Analysis of CRC in the animals at the end of the experiment showed that AOM/DSS induced CRC at a 75% incidence rate in WT mice receiving with PBS (6/8), 50% in WT mice treated with 5FU (4/8), a 100% incidence rate in both genotypes of TGF-β

signaling-deficient mice (8/8) (Table 1). Thus, the mutant mice had increased susceptibility to chemical-induced CRC.

Tumor phenotypes in *Smad4+/− Sptbn1+/−* and *Smad4+/−* mice were similar (Table 1, Table 3, Figure 2A, 2B) with a greater proportion of the more malignant form, adenocarcinoma than was observed in the WT mice that developed CRC (Figure 2B). Therefore, we grouped both genotypes together as TGF-β signaling-deficient group (SKO: *Smad4+/−Sptbn1+/−* and *Smad4+/−*). Histopathological analyses identified CRC tumors ranging from adenomas with low- or high-grade intraepithelial carcinoma-in-situ to frank adenocarcinomas in animals receiving PBS with WT mice developing tumors that were more frequently lower grade and the TGF-β signaling-deficient group developing higher-grade tumors at a significantly higher frequency ($p = 0.003$) (Table 2).

Not only were the TGF-β signaling-deficient group more susceptible to colitis-induced CRC that was more advanced, but this group was also developed a significantly increased number of tumors compared to WT mice, the individual tumors were also significantly larger in the combined mutant group compared to those in WT mice (Table 1), and the distribution of tumor sizes was also significantly different (Table 3). These results supported our hypothesis that TGF-β signaling deficiency contributes to CRC development and indicated that TGF-β signaling functions as a tumor suppressor at the early stage of CRC.

To determine if these findings with the mouse models were consistent with human CRC, we analyzed data from TCGA. More than 70% of human CRCs have *SMAD4* alterations (mutations and/or heterozygous loss) and a smaller fraction (8%) have mutations in *SPTBN1* (Figure 2C). Furthermore, these alterations correlated with significantly reduced disease-free survival (survival without progression of the disease) (Log-rank test, $p = 0.0169$) but not significantly different overall survival (the fact that the patient has not died from any cause) (Log-rank test, $p = 0.624$) (Figure 2C).

3.3 Colon tumors in TGF-β signaling-deficient mice exhibit chemoresistance to 5FU

TGF-β signaling defects have been linked with 5FU resistance [36, 51, 52]; therefore, we compared 4 weeks of 5FU treatment to PBS treatment and evaluated the drug response both in terms of tumor incidence and phenotypes and gut microbiome populations. None of the TGF-β signaling-deficient mice of either genotype had complete regression or absence of detectable tumors after 5FU treatment, whereas 4 out of 8 WT mice were completely tumor-free at the end of the treatment (Table 1). Additionally, the tumors in the TGF-β signaling-deficient group, which includes mice from both mutant genotypes, that had received 5FU treatment were more numerous and larger than those of the WT mice that received 5FU treatment (Figure 3A, 3B). There was also a significant difference ($p < 0.05$) in tumor size distribution between these two groups (Figure 3C). Although the TGF-β signaling-deficient group had a shift from predominantly large tumors after 5FU treatment, this 5FU-treated group had more animals with larger tumors sizes (80% at 2 – 3 mm and 10% at < 2 mm) than did the group of 5FU-treated WT animals (16.7% at 2 – 3 mm and 83.3% at < 2 mm) (Figure 3C, Table 3). Collectively, these results indicated that TGF-β signaling-deficient mice are more resistant to 5FU treatment of CRC compared to WT animals (Figure 3 and Table 1, Table 2, Table 3).

Analysis of human data showed that patients with *SMAD4* defects have reduced progression-free survival (Figure 2C). Consistent with this, we found that 1 of the TGF-β signaling-deficient mice (*Smad4+/−Sptbn1+/−*) developed colon cancer liver metastasis during 5FU treatment as confirmed by histopathological analysis (Figure 4). Although results from a single mouse are insufficient to draw a conclusion, this finding suggested that mutations associated with impaired or defective TGF-β signaling enhance tumor progression in CRC.

3.4 Proliferation is increased and apoptosis is decreased in tumors from TGF-β signaling-deficient mice

To investigate the molecular mechanism by which TGF-β deficiency contributes to tumor progression, we performed immunohistochemical analysis of cellular proliferation (Ki67) of the colonic tumors from WT and TGF-β signaling-deficient mice from both genotypes. We observed a significant increase in Ki67 index in the tumors of the TGF-β signaling-deficient group compared to the tumors of the WT mice (40.2 ± 3.5 vs 26.7 ± 3.4, $p < 0.05$) (Figure 5A–B). Moreover, we assessed the Ki67 index in normal adjacent colonic epithelial, which provides the environment for precancerous colonic hyperplasia. Our results suggested the normal adjacent colonic epithelium of mice in the TGF-β signaling-deficient group has a significantly increased Ki67 index (33.8 ± 2.6) compared to the same areas in WT mice (26.7 ± 3.3). Even when treated with 5FU, tumors from mice in the TGF-β signaling-deficient group (19.2 ± 3.6) had a significantly larger Ki67 index than tumors in the WT mice (6.2 ± 0.8) ($p < 0.05$) (Figure 5B). Thus, tumors from the TGF-β signaling-deficient group had a higher proliferation that was less affected by 5FU than the tumors in the WT mice.

We also evaluated if apoptosis differed between the groups by quantifying cells positive for cleaved caspase 3 (Figure 5C, D). We observed an increase in the number of cells positive for cleaved caspase 3 in the WT tumors from mice treated with 5FU compared with WT tumors from mice treated with PBS. In contrast, 5FU treatment failed to induce apoptosis in the tumors of the TGF-β signaling-deficient group. Collectively, the proliferation and apoptosis analyses suggested that enhanced proliferation and resistance to 5FU-induced apoptosis underlie the differences in tumor phenotypes between the WT and TGF-β signaling-deficient mice (Figure 5C, 5D).

3.5 Gut microbiome signatures associated with 5FU resistance and tumor progression were identified

Increasing evidence suggests that the human gut microbiome plays a critical role not only in tumor development but also in drug responsiveness. Thus, we performed shotgun metagenomic (Figure6A) sequencing using fecal samples from these mice to identify (i) changes in gut microbiota composition (eg. Family, Genus) (Figure6B–C) before and after tumor formation and (ii) changes in gut microbiota composition that correlated with 5FU response (Figure7). By analyzing the number and variety of bacterial species, we identified some species (*Enterocloster bolteae, Bacteroides dorei, Lachnoclostridium sp., and Mordavella sp. Marseille*) that had similar amounts in both WT mice and mice in the TGF-β signaling-deficient group, but these were significantly decreased after CRC induction

by AOM/DSS. This decrease after CRC induction was the same for WT mice and mice in the TGF-β signaling-deficient group. In contrast, 5FU treatment returned bacterial levels to pre-CRC levels in the WT group but not in the mice in the SKO group (Figure 7A). Among these bacteria, *Bacteroides dorei* is known to reduce LPS production and inhibit atherosclerosis [53], whereas *Lachnoclostridium sp.* was shown to be present in higher amounts in human colon adenoma [54]. Furthermore, our analysis revealed significantly decreased abundances of beneficial species following CRC induction in both WT mice and mice in the TGF-β signaling-deficient group (Figure 7B–C).

We also evaluated the bacteria associated with the tumors. Similar to the other Bacteroides species, their numbers recovered after 5FU treatment in tumors from WT mice but not in tumors from mice in the TGF-β signaling-deficient group. Most of these *Bacteroides* have anti-inflammatory effects and some are reported in colitis (e.g. *B. cellulosilyticus* [55], *B. Ovatus, B. Caccae* [56]) (Figure 7C). Surprisingly, Lactobacillus species commonly regarded as “anti-infective microbiomes”, had significantly increased levels in CRC animals but decreased upon 5FU treatment in WT mice. In mice in the TGF-β signaling-deficient group, the *Lactobacillus* species were also greater than that of the WT mice prior to tumor formation. After 5FU treatment, levels of *Lactobacillus* species were still greater in the mice in the TGF-β signaling-deficient group than in the WT mice. Although we are unable to conclude that *Lactobacillus* species are associated with 5FU resistance, at least 5FU treatment alone did not alter *Lactobacillus* species abundance. Rather the TGF-β signaling defect likely creates a microenvironment that allows the enrichment of *Lactobacillus species* regardless of tumor status (Figure7C).

4. Discussion

Our analyses revealed that TGF-β signaling-deficient mice had significantly increased numbers of certain bacterial species *(E. faecalis, A. finefoldii, A. shahii,, and Halomonas sp.*) and several significantly decreased gut microbiome species such as *B.vulgatus* and *P. distasonis*. Gut microorganisms in the GI tract play a critical role in cancer development and drug response [31–33, 57]. These bacteria, as well as others such as *Bacteroides vulgatus* and *Parabacteroides distasonis,* play an important role in multiple diseases. They are all significantly reduced in TGF-β signaling-deficient mice but have not been well studied in CRC [53, 58, 59]. Our studies suggest that our mice that are deficient in TGF-β signaling, spontaneously develop CRC in part through the modulation of the gut microbiome composition.

An increasing body of evidence has now linked gut microbiota to treatment response [31, 32, 57]. For example, *Fusobacterium nucleatum* (Fn), a well-known human CRC-associated microbe, contributes to oxaliplatin and 5-FU resistance through the regulation of autophagy, mediated by TLR4/MyD88/ miRNA-18a/ATG7 [33]. Crosstalk between TGF-β signaling and gut microbiome also plays a critical role in colon cancer development, because CRC fails to develop in germ-free mice with compromised signaling in the TGF-β pathway: Helicobacter infection is required to induce CRC in *Smad3*−/− mice and *Tgfb1*−/− mice, and germ-free *Tgfb1*−/− mice fail to develop CRC [30, 60]. Gut-microbial interaction and host-immune response play critical roles in creating an inflammatory environment

that contributes to colon cancer development with limited studies on drug resistance. In this study, our goal was to explore whether gut microbiota composition affects CRC chemotherapy response using mouse models. We also attempted to identify species or a unique gut microbiome signature(s) that can predict 5FU response. By identifying a species that is altered in the 5FU-resistant mice, one might be able to predict the response to 5FU or other interventions. There are a variety of CRC mouse models for exploring gut microbiome and drug response. However, we were interested in the primary changes of the gut microbiome and their contribution to non-cell-autonomous effects in tumor development and drug response. Therefore, we used *Smad4+/−* or *Smad4+/−Sptbn1+/−* mice rather than an orthotopic animal model, which adds more variabilities of the host immune response due to the implantation of human cell lines into mouse recipients [61]. Additionally, in human colon cancer, *SMAD4* deficiency contributes to 5FU resistance [36, 51, 52]. We found that tumors that developed in *Smad4+/−* or *Smad4+/−Sptbn1+/−* mice are more resistant to 5FU compared to tumors in WT mice. We identified a unique gut microbiome signature that is associated with 5FU resistance in mice in the mice in the TGF-β signaling-deficient group, comprised of both mutant genotypes. This is in contrast to our previous findings that a loss of TGF-β signaling through Sptbn1 knockdown in human cancer cell lines makes them more sensitive to 5FU. Considered together, these data suggest that 5FU resistance in tumors that develop in mice in the TGF-β signaling-deficient group represents a cell non-autonomous function of TGF-β signaling, which further emphasizes the importance of the contribution made by the gut microbiome and other microenvironmental factors to drug response [10, 33].

The TGF-β signaling pathway is a master regulator of gut microbiome homeostasis, inflammation, and the immune response [10, 15, 20, 27]. Our previous analysis of TGF-β signaling-deficient mice, comprised of *Smad4*+/− *Sptbn1*+/− mice and *Sptbn1*+/− mice, revealed that these mice had altered gut microbiome [10]. Comparing the results of the previous analysis with the results presented here revealed consistent changes in the gut microbiome across the two groups of TGF-β signaling-deficient mice, including increased amounts of species associated with human CRC and decreased amounts of species associated with a healthy microbiome. Collectively, these two studies provide strong support for the importance of TGF-β signaling in preventing the development of a cancer-permissive or cancer-promoting microbiome. At the molecular level, the unhealthy alteration in the gut microbiome that resulted from impaired TGF-β signaling likely involves both altered immune responses and the altered response of the colonic epithelium to bacteria. Indeed, the bacterial sensor protein CEACAM5 interacts with and inhibits the TGF-β receptor subunit TGFBR1 [10]. Future studies are required to determine the contribution of TGF-β-mediated effects on immune function and on the colonic epithelia in regulating the gut microbiome.

TGF-β deficiency, caused by *Smad4* deficiency, is associated with 5FU resistance [36, 51, 52]. Because we found that the *Smad4*+/− or *Smad4*+/− *Sptbn1*+/− mice exhibited similar microbiota profiles and tumor phenotypes, we combined the results from these mice as the TGF-β signaling-deficient group for statistical analyses. We used a model of AOM/DSS-induced CRC in mice in the TGF-β signaling-deficient group to explore the gut microbiome of mice with 5FU resistance. We identified unique bacterial species patterns related to the host's 5FU response. The abundances of *Enterocloster Boltae, Bacteroides*

dorei, Lachnoclostridium sp., and Mordavella sp. are markedly reduced in colon tumors. 5FU treatment returned these bacterial levels to normal in WT mice. However, 5FU treatment, failed to return these levels to normal in mice in the TGF-β signaling-deficient group. These data suggest that these bacterial species might be 5FU response-specific. Notably, Bacteroides is the major type of gut bacteria that is altered by 5FU in WT mice but not in mice in the TGF-β signaling-deficient group. This is not surprising, because Bacteroides species hydrolyze anti-viral drugs to a product that can inactivate an enzyme (dihydropyrimidine dehydrogenase) that detoxifies 5FU. This results in high 5FU levels that may be toxic to patients [62]. Potentially, measuring Bacteroides levels could be utilized for predicting a subject's response to 5-FU. Some of the Bacteroides species, such as *B. dorei, B. cellulosilyticus, B. ovatus,* and *B. caccae* are beneficial in that they possess anti-inflammatory effects [53, 56, 63]. This could have important clinical ramifications, insofar as 5FU remains the mainstay of chemotherapy for stage II and III CRC, yet over 30% of patients have 5FU resistance [64]. Future studies will determine whether evaluating the bacterial microbiome can be used for directing 5FU therapy. Additionally, we found that some bacterial species are altered by 5FU treatment; however, this response is not related to the host's TGF-β status [65]. For example, *Faecalibaculum _rodentium _strain_Alo17*, which is related to food digestion, is significantly reduced after 5FU treatment with no difference between WT mice and mice in the TGF-β signaling-deficient group. Levels of *Enterococcus_faecalis _strain_KUB3006* and *Turicibacter_sp._H121* are decreased by 5FU while levels of *Candidatus_arthromitu s_sp._SFB-mouse-NL* and *Alistipes_finegoldii_ strain_DSM_17242* are increased. Both changes occur regardless of the TGF-β signaling status of the host.

In summary, we and others have shown that mice defective in TGF-β signaling mice are more susceptible to CRC. As expected, we observed a larger number and a larger size of tumors in mice in the TGF-β signaling-deficient group as compared to the WT mice. The gut microbiome composition of mice in the TGF-β signaling-deficient group revealed a significantly different composition than that seen in WT mice. This observation suggests that certain microbiomes might be more prone to cancer development by providing a more permissible microenvironment for tumor development. We observed an increased abundance of *F. nucleatum* in the TGF-β signaling–defective mice, which is consistent with the previous report in human CRC [33] and our analysis of another group of TGF-β signaling–defective mice [10]. We observed substantially decreased levels of beneficial bacterial species, such as *B. vulgutus* [53] and *P. distasonis* [59, 66], in *Smad4+/−* deficient mice. However, these species are not altered by 5FU treatment, suggesting these microbiotas are related to CRC development but unlikely to be associated with drug response. In the current study, we applied a different platform and more stringent parameters for analysis than we used in our previous study [10] and we compared the effects of 5FU on WT and TGF-β signaling–defective mice. Thus, our current microbiome analyses revealed additional microbes that could be important for chemoresistance in humans. Surprisingly, *Lactobacillus* species commonly known to be beneficial, were increased in AOM/DSS-induced tumor, and decreased after 5FU treatment in WT mice but not in mice in the TGF-β signaling-deficient group. Potentially this could arise from a self-defense mechanism reflecting the host-immune response against the tumor; a follow-up study is required to determine whether

this is truly the case. Additionally, our study identified species related to food digestion, such as *Bacteroides_caecimuris_strain_I48, Faecalibaculum_rodentium_strain _Alo17*, were reduced after AOM/DSS treatment to induce CRC, suggesting that in human inflammation-associated CRC, disruption of the gut microbiome could impair normal food digestion.

Our data suggest that GI microorganisms altered in TGF-β signaling-deficient mice might significantly influence chemotherapeutic outcomes. Manipulating those species associated with 5FU resistance could potentially increase drug response. While it remains challenging to completely map the host microbiome, we believe manipulating the gut microbiome can be a promising therapeutic intervention for CRC.

Acknowledgments

We thank Kazufumi Ohshiro for sharing his ideas. We thank Nancy R. Gough with assistance in preparing the revised manuscript. We thank the sequencing service provided by Castle Raley in the Genomics Core at the George Washington University. We thank Charles Hadley King IV and Yao Ren for the initial development of the 2-step metagenomics analysis pipeline and continued support. This work was supported by NIH grants R01 AA023146 (L. Mishra), NIH R01 CA236591 (L. Mishra), NIH U01 CA230690 (L. Mishra), VA Merit I01BX003732 (L. Mishra), and GW CTR (L. Mishra), Elaine Snyder Award (L. Mishra), McCormick Genomic and Proteomic Center and GW Illumina/Genomics Core Mini-grant (SR, RM, LM).

Abbreviations:

CRC	Colorectal Cancer
TGF-β	Transforming Growth Factor β
TCGA	The Cancer Genome Atlas
TCGA-COAD	The Cancer Genome Atlas-Colorectal Adenocarcinoma
5FU	5-fluoro-uracil
PI3K	phosphoinositide 3-kinase
MAPK	mitogen-activated protein kinase

REFERENCES

[1]. Siegel RL, Miller KD, Goding Sauer A, Fedewa SA, Butterly LF, Anderson JC, Cercek A, Smith RA, Jemal A, Colorectal cancer statistics, 2020, CA Cancer J Clin 70(3) (2020) 145–164. [PubMed: 32133645]

[2]. Blaj C, Schmidt EM, Lamprecht S, Hermeking H, Jung A, Kirchner T, Horst D, Oncogenic Effects of High MAPK Activity in Colorectal Cancer Mark Progenitor Cells and Persist Irrespective of RAS Mutations, Cancer Res 77(7) (2017) 1763–1774. [PubMed: 28202525]

[3]. Li Y, Cao H, Jiao Z, Pakala SB, Sirigiri DN, Li W, Kumar R, Mishra L, Carcinoembryonic antigen interacts with TGF-{beta} receptor and inhibits TGF-{beta} signaling in colorectal cancers, Cancer Res 70(20) (2010) 8159–68. [PubMed: 20889724]

[4]. Mishra L, Shetty K, Tang Y, Stuart A, Byers SW, The role of TGF-beta and Wnt signaling in gastrointestinal stem cells and cancer, Oncogene 24(37) (2005) 5775–89. [PubMed: 16123810]

[5]. Pino MS, Chung DC, The chromosomal instability pathway in colon cancer, Gastroenterology 138(6) (2010) 2059–72. [PubMed: 20420946]

[6]. Reilly NM, Novara L, Di Nicolantonio F, Bardelli A, Exploiting DNA repair defects in colorectal cancer, Mol Oncol 13(4) (2019) 681–700. [PubMed: 30714316]

[7]. Solomon H, Dinowitz N, Pateras IS, Cooks T, Shetzer Y, Molchadsky A, Charni M, Rabani S, Koifman G, Tarcic O, Porat Z, Kogan-Sakin I, Goldfinger N, Oren M, Harris CC, Gorgoulis VG, Rotter V, Mutant p53 gain of function underlies high expression levels of colorectal cancer stem cells markers, Oncogene 37(12) (2018) 1669–1684. [PubMed: 29343849]

[8]. Vinson KE, George DC, Fender AW, Bertrand FE, Sigounas G, The Notch pathway in colorectal cancer, Int J Cancer 138(8) (2016) 1835–42. [PubMed: 26264352]

[9]. Grady WM, Markowitz SD, Genetic and epigenetic alterations in colon cancer, Annu Rev Genomics Hum Genet 3 (2002) 101–28. [PubMed: 12142355]

[10]. Gu S, Zaidi S, Hassan MI, Mohammad T, Malta TM, Noushmehr H, Nguyen B, Crandall KA, Srivastav J, Obias V, Lin P, Nguyen BN, Yao M, Yao R, King CH, Mazumder R, Mishra B, Rao S, Mishra L, Mutated CEACAMs Disrupt Transforming Growth Factor Beta Signaling and Alter the Intestinal Microbiome to Promote Colorectal Carcinogenesis, Gastroenterology 158(1) (2020) 238–252. [PubMed: 31585122]

[11]. N. Cancer Genome Atlas, Comprehensive molecular characterization of human colon and rectal cancer, Nature 487(7407) (2012) 330–7. [PubMed: 22810696]

[12]. Akhurst RJ, Targeting TGF-beta Signaling for Therapeutic Gain, Cold Spring Harb Perspect Biol 9(10) (2017).

[13]. Calon A, Espinet E, Palomo-Ponce S, Tauriello DV, Iglesias M, Cespedes MV, Sevillano M, Nadal C, Jung P, Zhang XH, Byrom D, Riera A, Rossell D, Mangues R, Massague J, Sancho E, Batlle E, Dependency of colorectal cancer on a TGF-beta-driven program in stromal cells for metastasis initiation, Cancer Cell 22(5) (2012) 571–84. [PubMed: 23153532]

[14]. Tang Y, Katuri V, Srinivasan R, Fogt F, Redman R, Anand G, Said A, Fishbein T, Zasloff M, Reddy EP, Mishra B, Mishra L, Transforming growth factor-beta suppresses nonmetastatic colon cancer through Smad4 and adaptor protein ELF at an early stage of tumorigenesis, Cancer Res 65(10) (2005) 4228–37. [PubMed: 15899814]

[15]. Tauriello DVF, Palomo-Ponce S, Stork D, Berenguer-Llergo A, Badia-Ramentol J, Iglesias M, Sevillano M, Ibiza S, Canellas A, Hernando-Momblona X, Byrom D, Matarin JA, Calon A, Rivas EI, Nebreda AR, Riera A, Attolini CS, Batlle E, TGFbeta drives immune evasion in genetically reconstituted colon cancer metastasis, Nature 554(7693) (2018) 538–543. [PubMed: 29443964]

[16]. Morikawa M, Derynck R, Miyazono K, TGF-beta and the TGF-beta Family: Context-Dependent Roles in Cell and Tissue Physiology, Cold Spring Harb Perspect Biol 8(5) (2016).

[17]. Korkut A, Zaidi S, Kanchi RS, Rao S, Gough NR, Schultz A, Li X, Lorenzi PL, Berger AC, Robertson G, Kwong LN, Datto M, Roszik J, Ling S, Ravikumar V, Manyam G, Rao A, Shelley S, Liu Y, Ju Z, Hansel D, de Velasco G, Pennathur A, Andersen JB, O'Rourke CJ, Ohshiro K, Jogunoori W, Nguyen BN, Li S, Osmanbeyoglu HU, Ajani JA, Mani SA, Houseman A, Wiznerowicz M, Chen J, Gu S, Ma W, Zhang J, Tong P, Cherniack AD, Deng C, Resar L, N. Cancer Genome Atlas Research, Weinstein JN, Mishra L, Akbani R, A Pan-Cancer Analysis Reveals High-Frequency Genetic Alterations in Mediators of Signaling by the TGF-beta Superfamily, Cell Syst 7(4) (2018) 422–437 e7. [PubMed: 30268436]

[18]. Rao S, Zaidi S, Banerjee J, Jogunoori W, Sebastian R, Mishra B, Nguyen B-N, Wu RC, White J, Deng C, Amdur R, Li S, Mishra L, Transforming Growth Factor-β in Liver Cancer Stem Cells and Regeneration, Hepatology Communications 1(6) (2017) 477–493. [PubMed: 29404474]

[19]. Massague J, TGFbeta in Cancer, Cell 134(2) (2008) 215–30. [PubMed: 18662538]

[20]. Massague J, TGFbeta signalling in context, Nat Rev Mol Cell Biol 13(10) (2012) 616–30. [PubMed: 22992590]

[21]. Zhang Y, Alexander PB, Wang XF, TGF-beta Family Signaling in the Control of Cell Proliferation and Survival, Cold Spring Harb Perspect Biol 9(4) (2017).

[22]. Guo X, Wang XF, Signaling cross-talk between TGF-beta/BMP and other pathways, Cell Res 19(1) (2009) 71–88. [PubMed: 19002158]

[23]. Okugawa Y, Grady WM, Goel A, Epigenetic Alterations in Colorectal Cancer: Emerging Biomarkers, Gastroenterology 149(5) (2015) 1204–1225 e12. [PubMed: 26216839]

[24]. Hoosein NM, McKnight MK, Levine AE, Mulder KM, Childress KE, Brattain DE, Brattain MG, Differential sensitivity of subclasses of human colon carcinoma cell lines to the growth inhibitory

effects of transforming growth factor-beta 1, Exp Cell Res 181(2) (1989) 442–53. [PubMed: 2538337]

[25]. Akhurst RJ, TGF beta signaling in health and disease, Nat Genet 36(8) (2004) 790–2. [PubMed: 15284845]

[26]. Chen J, Zaidi S, Rao S, Chen JS, Phan L, Farci P, Su X, Shetty K, White J, Zamboni F, Wu X, Rashid A, Pattabiraman N, Mazumder R, Horvath A, Wu RC, Li S, Xiao C, Deng CX, Wheeler DA, Mishra B, Akbani R, Mishra L, Analysis of Genomes and Transcriptomes of Hepatocellular Carcinomas Identifies Mutations and Gene Expression Changes in the Transforming Growth Factor-beta Pathway, Gastroenterology 154(1) (2018) 195–210. [PubMed: 28918914]

[27]. Bauche D, Marie JC, Transforming growth factor beta: a master regulator of the gut microbiota and immune cell interactions, Clin Transl Immunology 6(4) (2017) e136. [PubMed: 28523126]

[28]. Konkel JE, Chen W, Balancing acts: the role of TGF-beta in the mucosal immune system, Trends Mol Med 17(11) (2011) 668–76. [PubMed: 21890412]

[29]. Wong SH, Yu J, Gut microbiota in colorectal cancer: mechanisms of action and clinical applications, Nat Rev Gastroenterol Hepatol 16(11) (2019) 690–704. [PubMed: 31554963]

[30]. Engle SJ, Ormsby I, Pawlowski S, Boivin GP, Croft J, Balish E, Doetschman T, Elimination of colon cancer in germ-free transforming growth factor beta 1-deficient mice, Cancer Res 62(22) (2002) 6362–6. [PubMed: 12438215]

[31]. Alexander JL, Wilson ID, Teare J, Marchesi JR, Nicholson JK, Kinross JM, Gut microbiota modulation of chemotherapy efficacy and toxicity, Nat Rev Gastroenterol Hepatol 14(6) (2017) 356–365. [PubMed: 28270698]

[32]. Ramos A, Hemann MT, Drugs, Bugs, and Cancer: Fusobacterium nucleatum Promotes Chemoresistance in Colorectal Cancer, Cell 170(3) (2017) 411–413. [PubMed: 28753421]

[33]. Yu T, Guo F, Yu Y, Sun T, Ma D, Han J, Qian Y, Kryczek I, Sun D, Nagarsheth N, Chen Y, Chen H, Hong J, Zou W, Fang JY, Fusobacterium nucleatum Promotes Chemoresistance to Colorectal Cancer by Modulating Autophagy, Cell 170(3) (2017) 548–563 e16. [PubMed: 28753429]

[34]. Cerami E, Gao J, Dogrusoz U, Gross BE, Sumer SO, Aksoy BA, Jacobsen A, Byrne CJ, Heuer ML, Larsson E, Antipin Y, Reva B, Goldberg AP, Sander C, Schultz N, The cBio cancer genomics portal: an open platform for exploring multidimensional cancer genomics data, Cancer Discov 2(5) (2012) 401–4. [PubMed: 22588877]

[35]. Miyaki M, Iijima T, Konishi M, Sakai K, Ishii A, Yasuno M, Hishima T, Koike M, Shitara N, Iwama T, Utsunomiya J, Kuroki T, Mori T, Higher frequency of Smad4 gene mutation in human colorectal cancer with distant metastasis, Oncogene 18(20) (1999) 3098–103. [PubMed: 10340381]

[36]. Alhopuro P, Alazzouzi H, Sammalkorpi H, Davalos V, Salovaara R, Hemminki A, Jarvinen H, Mecklin JP, Schwartz S Jr., Aaltonen LA, Arango D, SMAD4 levels and response to 5-fluorouracil in colorectal cancer, Clin Cancer Res 11(17) (2005) 6311–6. [PubMed: 16144935]

[37]. Baraniskin A, Munding J, Schulmann K, Meier D, Porschen R, Arkenau HT, Graeven U, Schmiegel W, Tannapfel A, Reinacher-Schick A, Prognostic value of reduced SMAD4 expression in patients with metastatic colorectal cancer under oxaliplatin-containing chemotherapy: a translational study of the AIO colorectal study group, Clin Colorectal Cancer 10(1) (2011) 24–9. [PubMed: 21609932]

[38]. Neufert C, Becker C, Neurath MF, An inducible mouse model of colon carcinogenesis for the analysis of sporadic and inflammation-driven tumor progression, Nat Protoc 2(8) (2007) 1998–2004. [PubMed: 17703211]

[39]. Means AL, Freeman TJ, Zhu J, Woodbury LG, Marincola-Smith P, Wu C, Meyer AR, Weaver CJ, Padmanabhan C, An H, Zi J, Wessinger BC, Chaturvedi R, Brown TD, Deane NG, Coffey RJ, Wilson KT, Smith JJ, Sawyers CL, Goldenring JR, Novitskiy SV, Washington MK, Shi C, Beauchamp RD, Epithelial Smad4 Deletion Up-Regulates Inflammation and Promotes Inflammation-Associated Cancer, Cell Mol Gastroenterol Hepatol 6(3) (2018) 257–276. [PubMed: 30109253]

[40]. Al-Greene NT, Means AL, Lu P, Jiang A, Schmidt CR, Chakravarthy AB, Merchant NB, Washington MK, Zhang B, Shyr Y, Deane NG, Beauchamp RD, Four jointed box 1 promotes

angiogenesis and is associated with poor patient survival in colorectal carcinoma, PLoS One 8(7) (2013) e69660. [PubMed: 23922772]

[41]. Song MK, Park MY, Sung MK, 5-Fluorouracil-induced changes of intestinal integrity biomarkers in BALB/c mice, J Cancer Prev 18(4) (2013) 322–9. [PubMed: 25337561]

[42]. Rao S, Peri S, Hoffmann J, Cai KQ, Harris B, Rhodes M, Connolly DC, Testa JR, Wiest DL, RPL22L1 induction in colorectal cancer is associated with poor prognosis and 5-FU resistance, PLoS One 14(10) (2019) e0222392. [PubMed: 31581233]

[43]. Rivera M, Fichtner I, Wulf-Goldenberg A, Sers C, Merk J, Patone G, Alp KM, Kanashova T, Mertins P, Hoffmann J, Stein U, Walther W, Patient-derived xenograft (PDX) models of colorectal carcinoma (CRC) as a platform for chemosensitivity and biomarker analysis in personalized medicine, Neoplasia 23(1) (2021) 21–35. [PubMed: 33212364]

[44]. Simonyan V, Mazumder R, High-Performance Integrated Virtual Environment (HIVE) Tools and Applications for Big Data Analysis, Genes (Basel) 5(4) (2014) 957–81. [PubMed: 25271953]

[45]. King CH, Desai H, Sylvetsky AC, LoTempio J, Ayanyan S, Carrie J, Crandall KA, Fochtman BC, Gasparyan L, Gulzar N, Howell P, Issa N, Krampis K, Mishra L, Morizono H, Pisegna JR, Rao S, Ren Y, Simonyan V, Smith K, VedBrat S, Yao MD, Mazumder R, Baseline human gut microbiota profile in healthy people and standard reporting template, PLoS One 14(9) (2019) e0206484. [PubMed: 31509535]

[46]. Santana-Quintero L, Dingerdissen H, Thierry-Mieg J, Mazumder R, Simonyan V, HIVE-hexagon: high-performance, parallelized sequence alignment for next-generation sequencing data analysis, PLoS One 9(6) (2014) e99033. [PubMed: 24918764]

[47]. UniProt C, UniProt: a worldwide hub of protein knowledge, Nucleic Acids Res 47(D1) (2019) D506–D515. [PubMed: 30395287]

[48]. Shamsaddini A, Pan Y, Johnson WE, Krampis K, Shcheglovitova M, Simonyan V, Zanne A, Mazumder R, Census-based rapid and accurate metagenome taxonomic profiling, BMC Genomics 15 (2014) 918. [PubMed: 25336203]

[49]. Nambiar PR, Girnun G, Lillo NA, Guda K, Whiteley HE, Rosenberg DW, Preliminary analysis of azoxymethane induced colon tumors in inbred mice commonly used as transgenic/knockout progenitors, Int J Oncol 22(1) (2003) 145–50. [PubMed: 12469197]

[50]. Suzuki R, Kohno H, Sugie S, Nakagama H, Tanaka T, Strain differences in the susceptibility to azoxymethane and dextran sodium sulfate-induced colon carcinogenesis in mice, Carcinogenesis 27(1) (2006) 162–9. [PubMed: 16081511]

[51]. Zhang B, Zhang B, Chen X, Bae S, Singh K, Washington MK, Datta PK, Loss of Smad4 in colorectal cancer induces resistance to 5-fluorouracil through activating Akt pathway, Br J Cancer 110(4) (2014) 946–57. [PubMed: 24384683]

[52]. Wong CK, Lambert AW, Ozturk S, Papageorgis P, Lopez D, Shen N, Sen Z, Abdolmaleky HM, Gyorffy B, Feng H, Thiagalingam S, Targeting RICTOR Sensitizes SMAD4-Negative Colon Cancer to Irinotecan, Mol Cancer Res 18(3) (2020) 414–423. [PubMed: 31932471]

[53]. Yoshida N, Emoto T, Yamashita T, Watanabe H, Hayashi T, Tabata T, Hoshi N, Hatano N, Ozawa G, Sasaki N, Mizoguchi T, Amin HZ, Hirota Y, Ogawa W, Yamada T, Hirata KI, Bacteroides vulgatus and Bacteroides dorei Reduce Gut Microbial Lipopolysaccharide Production and Inhibit Atherosclerosis, Circulation 138(22) (2018) 2486–2498. [PubMed: 30571343]

[54]. Liang JQ, Li T, Nakatsu G, Chen YX, Yau TO, Chu E, Wong S, Szeto CH, Ng SC, Chan FKL, Fang JY, Sung JJY, Yu J, A novel faecal Lachnoclostridium marker for the non-invasive diagnosis of colorectal adenoma and cancer, Gut 69(7) (2020) 1248–1257. [PubMed: 31776231]

[55]. Neff CP, Rhodes ME, Arnolds KL, Collins CB, Donnelly J, Nusbacher N, Jedlicka P, Schneider JM, McCarter MD, Shaffer M, Mazmanian SK, Palmer BE, Lozupone CA, Diverse Intestinal Bacteria Contain Putative Zwitterionic Capsular Polysaccharides with Anti-inflammatory Properties, Cell Host Microbe 20(4) (2016) 535–547. [PubMed: 27693306]

[56]. Hiippala K, Kainulainen V, Suutarinen M, Heini T, Bowers JR, Jasso-Selles D, Lemmer D, Valentine M, Barnes R, Engelthaler DM, Satokari R, Isolation of Anti-Inflammatory and Epithelium Reinforcing Bacteroides and Parabacteroides Spp. from A Healthy Fecal Donor, Nutrients 12(4) (2020).

[57]. Gopalakrishnan V, Spencer CN, Nezi L, Reuben A, Andrews MC, Karpinets TV, Prieto PA, Vicente D, Hoffman K, Wei SC, Cogdill AP, Zhao L, Hudgens CW, Hutchinson DS, Manzo T, Petaccia de Macedo M, Cotechini T, Kumar T, Chen WS, Reddy SM, Szczepaniak Sloane R, Galloway-Pena J, Jiang H, Chen PL, Shpall EJ, Rezvani K, Alousi AM, Chemaly RF, Shelburne S, Vence LM, Okhuysen PC, Jensen VB, Swennes AG, McAllister F, Marcelo Riquelme Sanchez E, Zhang Y, Le Chatelier E, Zitvogel L, Pons N, Austin-Breneman JL, Haydu LE, Burton EM, Gardner JM, Sirmans E, Hu J, Lazar AJ, Tsujikawa T, Diab A, Tawbi H, Glitza IC, Hwu WJ, Patel SP, Woodman SE, Amaria RN, Davies MA, Gershenwald JE, Hwu P, Lee JE, Zhang J, Coussens LM, Cooper ZA, Futreal PA, Daniel CR, Ajami NJ, Petrosino JF, Tetzlaff MT, Sharma P, Allison JP, Jenq RR, Wargo JA, Gut microbiome modulates response to anti-PD-1 immunotherapy in melanoma patients, Science 359(6371) (2018) 97–103. [PubMed: 29097493]

[58]. O.C. P, de Wouters T, Giri R, Mondot S, Smith WJ, Blottiere HM, Begun J, Morrison M, The gut bacterium and pathobiont Bacteroides vulgatus activates NF-kappaB in a human gut epithelial cell line in a strain and growth phase dependent manner, Anaerobe 47 (2017) 209–217. [PubMed: 28583864]

[59]. Wang K, Liao M, Zhou N, Bao L, Ma K, Zheng Z, Wang Y, Liu C, Wang W, Wang J, Liu SJ, Liu H, Parabacteroides distasonis Alleviates Obesity and Metabolic Dysfunctions via Production of Succinate and Secondary Bile Acids, Cell Rep 26(1) (2019) 222–235 e5. [PubMed: 30605678]

[60]. Maggio-Price L, Treuting P, Zeng W, Tsang M, Bielefeldt-Ohmann H, Iritani BM, Helicobacter infection is required for inflammation and colon cancer in SMAD3-deficient mice, Cancer Res 66(2) (2006) 828–38. [PubMed: 16424015]

[61]. Chen YC, Miao ZF, Yip KL, Cheng YA, Liu CJ, Li LH, Lin CY, Wang JW, Wu DC, Cheng TL, Wang JY, Gut Fecal Microbiota Transplant in a Mouse Model of Orthotopic Rectal Cancer, Front Oncol 10 (2020) 568012. [PubMed: 33194651]

[62]. Nakayama H, Kinouchi T, Kataoka K, Akimoto S, Matsuda Y, Ohnishi Y, Intestinal anaerobic bacteria hydrolyse sorivudine, producing the high blood concentration of 5-(E)-(2-bromovinyl)uracil that increases the level and toxicity of 5-fluorouracil, Pharmacogenetics 7(1) (1997) 35–43. [PubMed: 9110360]

[63]. Tan H, Zhao J, Zhang H, Zhai Q, Chen W, Novel strains of Bacteroides fragilis and Bacteroides ovatus alleviate the LPS-induced inflammation in mice, Appl Microbiol Biotechnol 103(5) (2019) 2353–2365. [PubMed: 30666361]

[64]. Sargent D, Sobrero A, Grothey A, O'Connell MJ, Buyse M, Andre T, Zheng Y, Green E, Labianca R, O'Callaghan C, Seitz JF, Francini G, Haller D, Yothers G, Goldberg R, de Gramont A, Evidence for cure by adjuvant therapy in colon cancer: observations based on individual patient data from 20,898 patients on 18 randomized trials, J Clin Oncol 27(6) (2009) 872–7. [PubMed: 19124803]

[65]. Yuan L, Zhang S, Li H, Yang F, Mushtaq N, Ullah S, Shi Y, An C, Xu J, The influence of gut microbiota dysbiosis to the efficacy of 5-Fluorouracil treatment on colorectal cancer, Biomed Pharmacother 108 (2018) 184–193. [PubMed: 30219675]

[66]. Koh GY, Kane A, Lee K, Xu Q, Wu X, Roper J, Mason JB, Crott JW, Parabacteroides distasonis attenuates toll-like receptor 4 signaling and Akt activation and blocks colon tumor formation in high-fat diet-fed azoxymethane-treated mice, Int J Cancer 143(7) (2018) 1797–1805. [PubMed: 29696632]

Highlights:

- Mice with defective TGF-β signaling are more susceptible to chemically-induced CRC
- CRC that develops in mice with defective TGF-β signaling is resistant to 5FU
- Mice with defective TGF-β signaling display an altered gut microbiome signature
- 5FU resistance correlates with imbalanced intestinal microbial populations

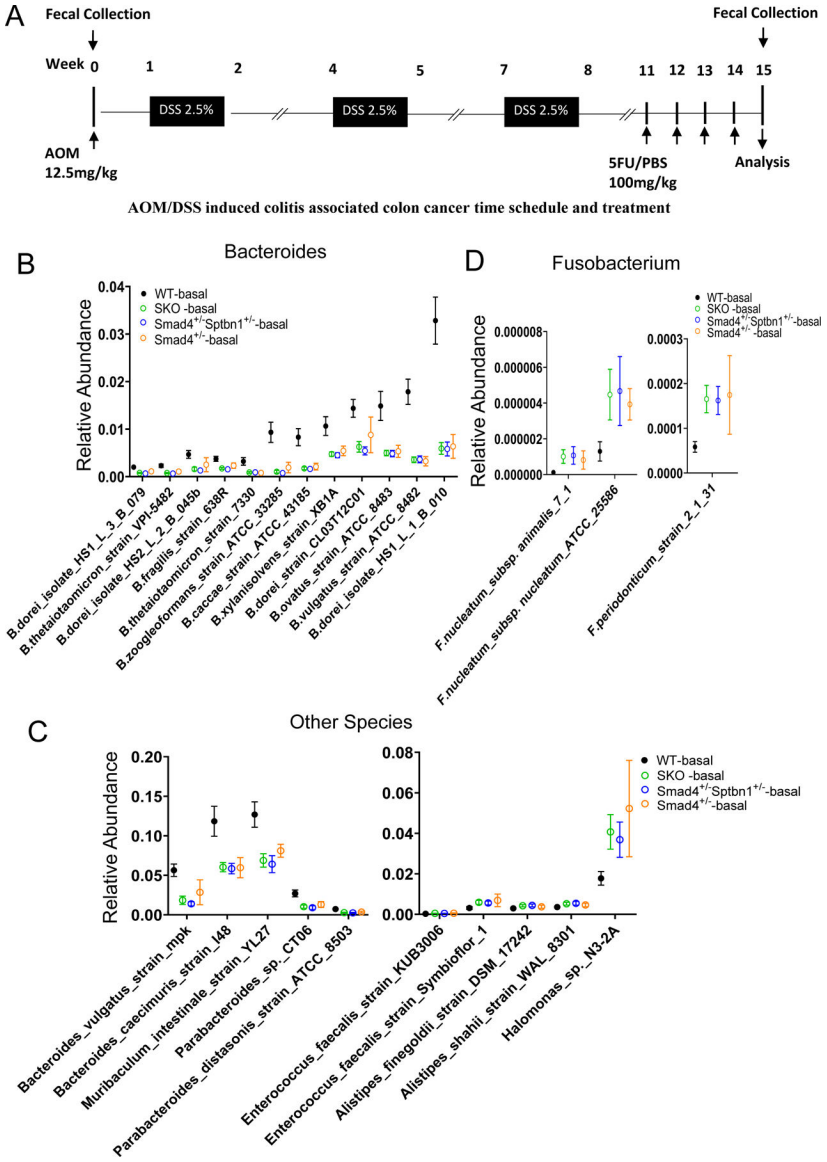

Figure 1.

Significantly altered basal proportions of gut microbiota species in TGF-β signaling-deficient mice (SKO: *Smad4+/–/Sptbn1+/–* and Smad4+/−). (A) Schematic of AOM/DSS-induced CRC mouse model to explore 5FU response and gut microbiome in WT (n = 16), *Smad4+/–Sptbn1+/–* (n = 12), and *Smad4*+/− (n = 4) mice. Fecal samples were collected before CRC induction (basal) and after CRC induction and drug or control treatment (5FU or PBS) at Week 15. (B – D) Relative abundances of bacteria in mice of the indicated genotypes of mice before any treatment (basal). SKO (n = 16), combined results from *Smad4*+/–*Sptbn1*+/– (n = 12) and *Smad4*+/− (n = 4). Data are shown as the average ± SEM. Species shown in B-C are those that exhibited $p < 0.01$ between WT and *Smad4+/–Sptbn1+/–* or WT and SKO as determined by unpaired *t-test*. Fusobacterium species (D) exhibited $p < 0.05$ between WT and SKO, or *Smad4+/–Sptbn1+/–* or *Smad4+/–* as determined by unpaired *t-test*.

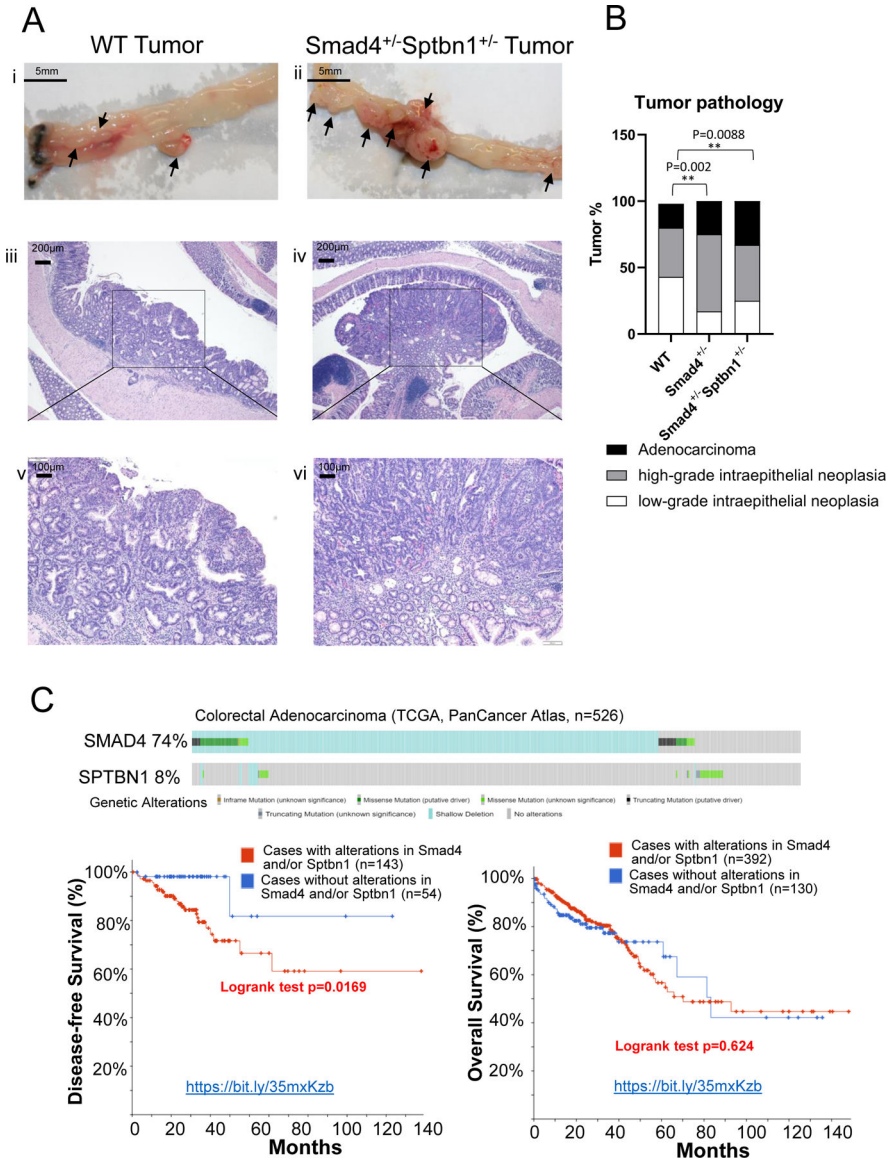

Figure 2.

Smad4+/– and *Smad4+/–/Sptbn1+/–* mice are more susceptible to AOM/DSS-induced CRC. (A) Representative colon tumors (top, arrow) and pathological analysis by hematoxylin-eosin staining (middle and bottom) in a WT mouse (left) and *Smad4+/–/Sptbn1+/–* mouse (right). WT mice colon tumor was diagnosed as a high-grade adenoma (i, iii, and v); *Smad4+/–/Sptbn1+/–* colon tumor was diagnosed as a moderately differentiated adenocarcinoma (ii, iv, and vi). Scale bars, 5 mm, 200 μm, and 100 μm. (B) Bar graph showing summary of histopathological analyses of tumors from TGF-β signaling-deficient mice [*Smad4+/–/Sptbn1+/–* (n = 5), *Smad4+/−* (n = 3)] and WT mice (n = 6). Significance testing was performed with Chi-square. (C) Onco-Prints of genomic alterations of *SMAD4* and *SPTBN1* from TCGA CRC data (n = 526) (top). Kaplan-Meier survival plots of patients stratified according to genetic alterations of *SMAD4* and *SPTBN1* including Disease-free

survival (bottom left) and overall (bottom-right) survival, the P values were calculated by log-rank test.

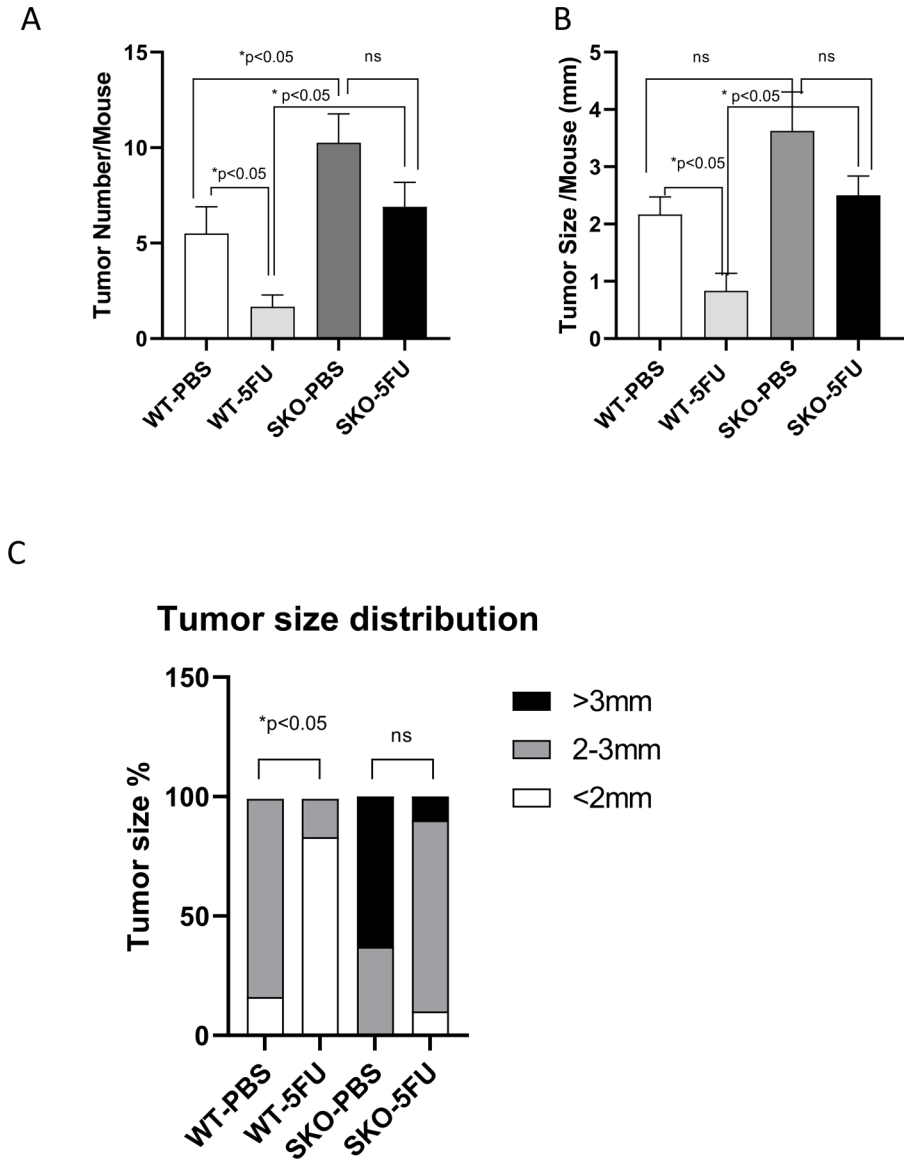

Figure 3.

Smad4+/– and *Smad4+/–/Sptbn1+/–* tumors are resistant to 5FU. (A) Mice that are deficient in TGF-β signaling (SKO: *Smad4+/–/Sptbn1+/–* and Smad4+/−) display significantly increased tumor numbers compared to WT mice. 5FU treatment significantly reduced tumor numbers in WT mice, but not in TGF-β signaling-deficient mice. Significance was performed using an unpaired t-test. (B) SKO mice show the trend of enlarged tumor size compared to WT mice. 5FU treatment significantly reduced tumor size in WT mice, but not in SKO mice. Significance was performed using an unpaired t-test. (C) Tumor size distribution analysis indicated significantly decreased tumor size in WT tumor after 5FU treatment, but no statistical tumor size differences in SKO tumor after 5FU treatment. Significance was performed using Chi-square, *p < 0.05. WT-PBS, n = 6; WT-5FU, n = 6; SKO-PBS (n = 5, *Smad4+/–Sptbn1+/–; n = 3, Smad4+/–*); SKO-5FU, (n = 7, *Smad4+/–Sptbn1+/–; n = 3, Smad4+/–*).

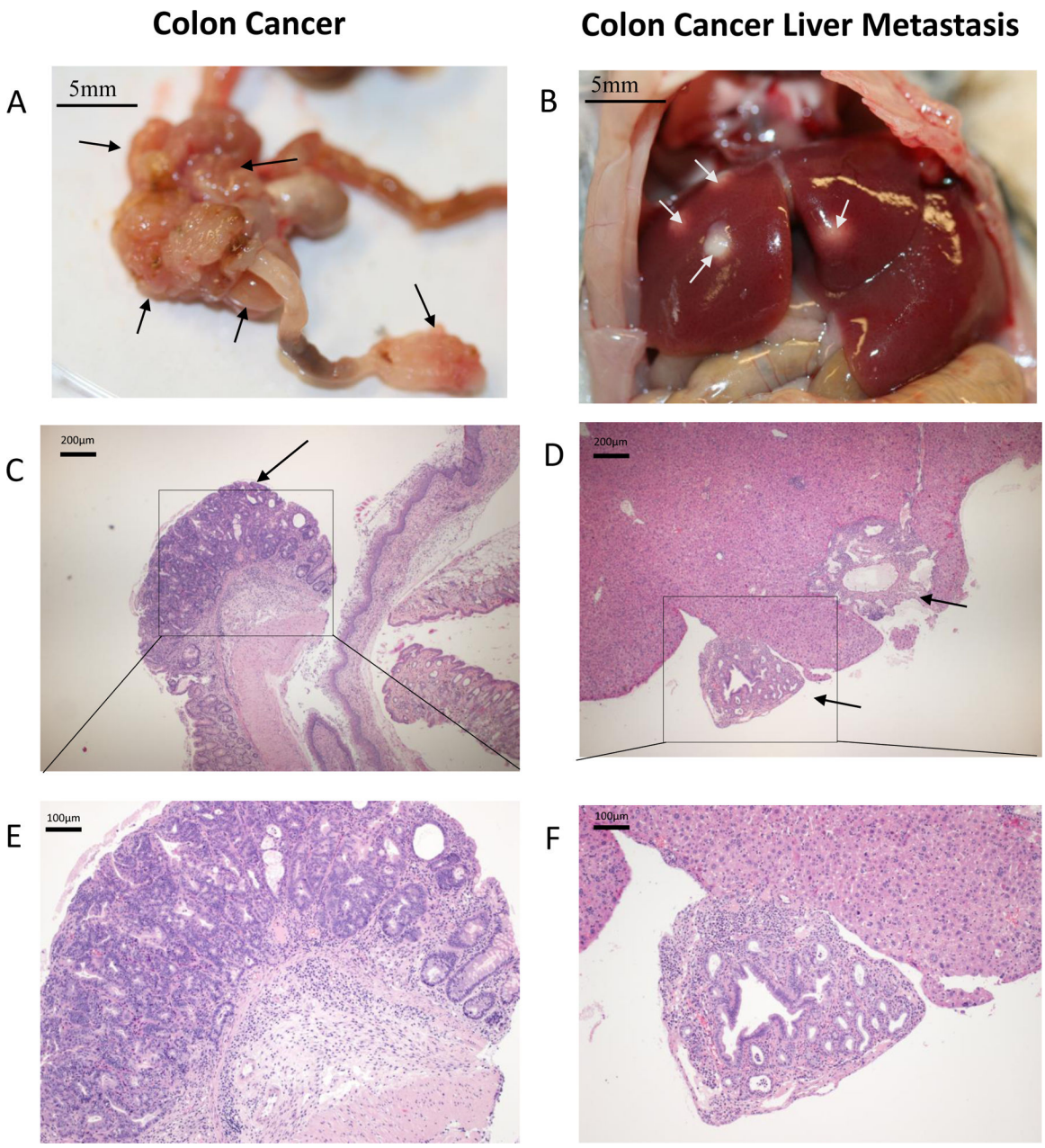

Figure 4.

Smad4+/–/Sptbn1+/– tumor after 5FU treatment progresses to liver metastasis. Gross view of primary colon tumors (A) and liver metastasis (B). The histopathological assessment confirmed the tumors in A are primary CRC (C, E) and tumor nodules shown in the B are colon cancer liver metastasis (D, F). Scale bars, 5 mm, 200 μm and 100um.

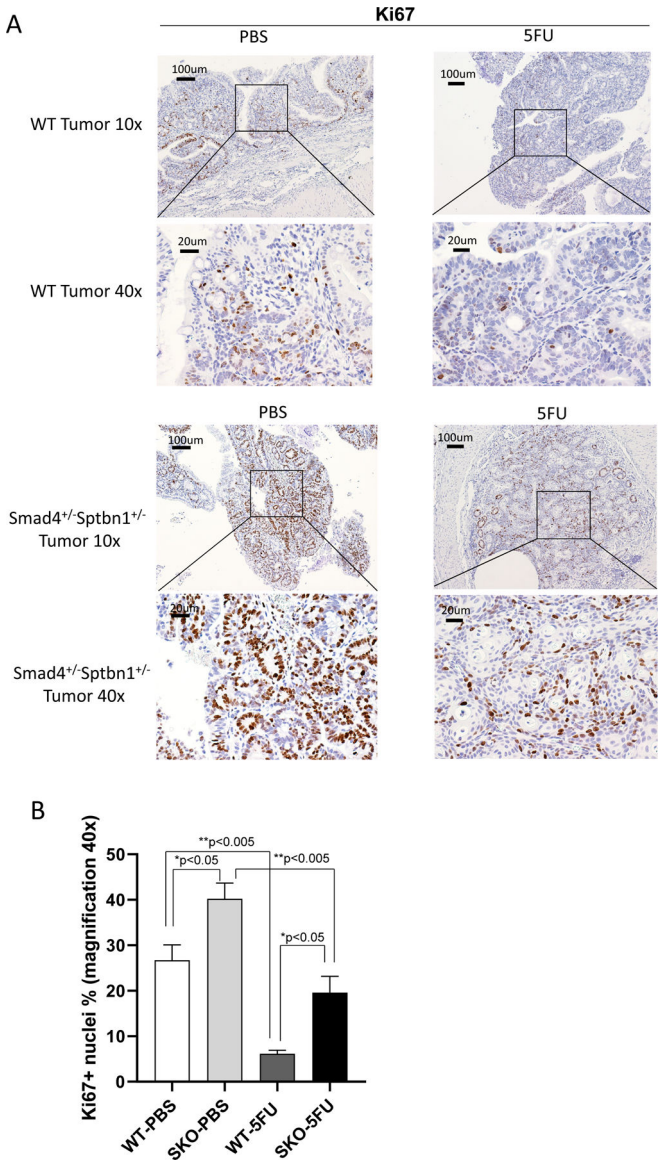

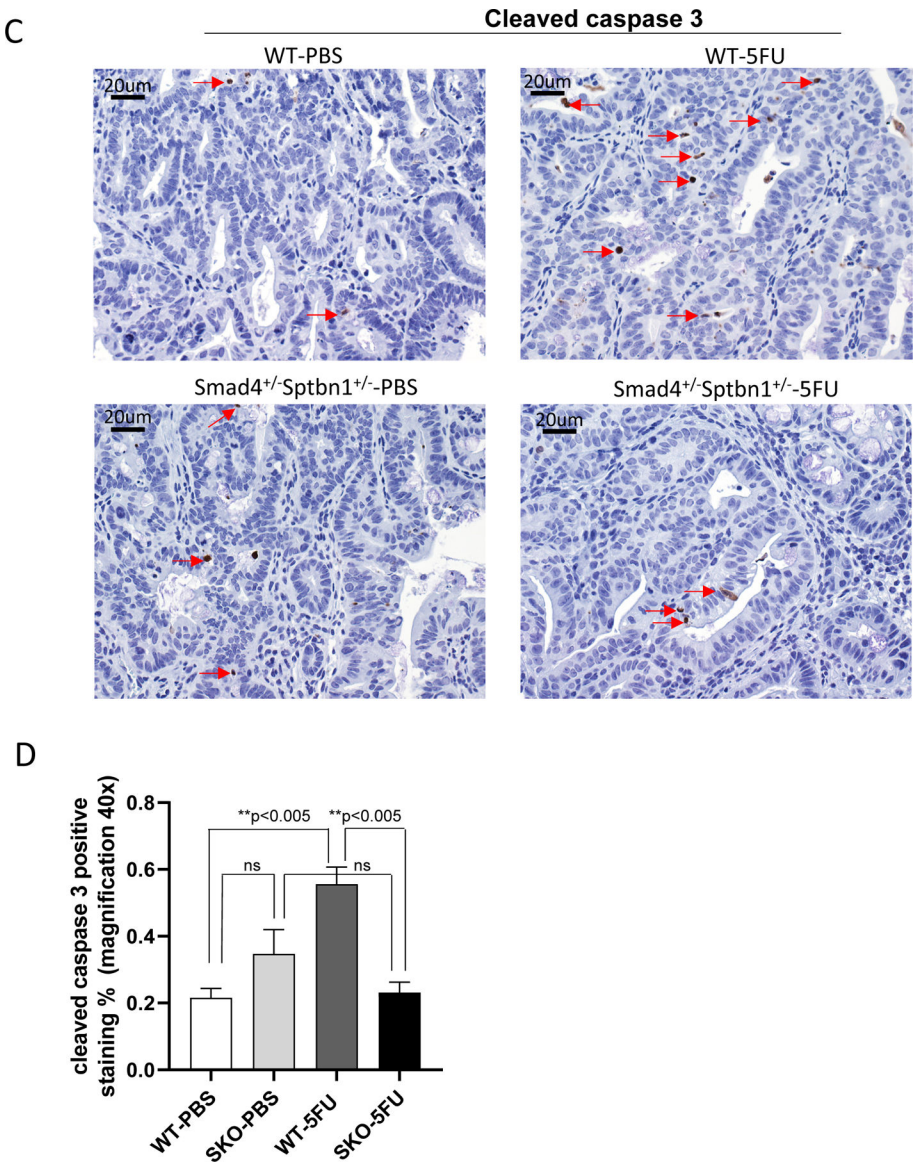

Figure 5.

Proliferation and apoptosis in TGF-β signaling–deficient tumors by Ki67 and cleaved caspase 3 immunohistochemistry. (A) Representative colon sections from WT and *Smad4+/–/Sptbn1+/–* mice stained for Ki67. Scale bars, 100 μm, and 20 μm. The percentage of Ki67+ nuclei per field (5 randomly selected fields) was determined. (B) 5FU treatment significantly decreased the Ki67 index in both WT and TGF-β signaling–deficient colon tumors. Compared to the WT colon tumor, TGF-β signaling–deficient colon tumor showed a significantly higher Ki67 index even after 5FU treatment. (C-D) Representative colon sections from each group with positive staining of cleaved caspase-3 (arrows) and quantification of the number of cells with positive staining of cleaved caspase-3. Significance was performed using a one-way ANOVA test for 4 groups comparison in B ($p < 0.0001$) and D ($p = 0.0013$). In B, by Bonferroni's multiple comparisons test for Ki67: **p<0.005 for WT-PBS vs. WT-5FU; *p<0.05 for SKO-PBS vs. WT-PBS;

**p<0.005 for SKO-PBS vs. SKO-5FU; *p<0.05 for WT-5FU vs SKO-5FU. In D, by Bonferroni's multiple comparisons test for caspase 3: **p<0.005 for WT-PBS vs. WT-5FU; no significance between SKO-PBS vs. WT-PBS or between SKO-PBS vs SKO-5FU; **p<0.005 for WT-5FU vs SKO-5FU. WT-PBS, n = 6; WT-5FU, n = 6; SKO -PBS (n = 5, *Smad4+/−Sptbn1+/−;* n = 3, *Smad4+/−*); SKO −5FU, (n = 7, *Smad4+/−Sptbn1+/−;* n = 3, *Smad4+/−*).

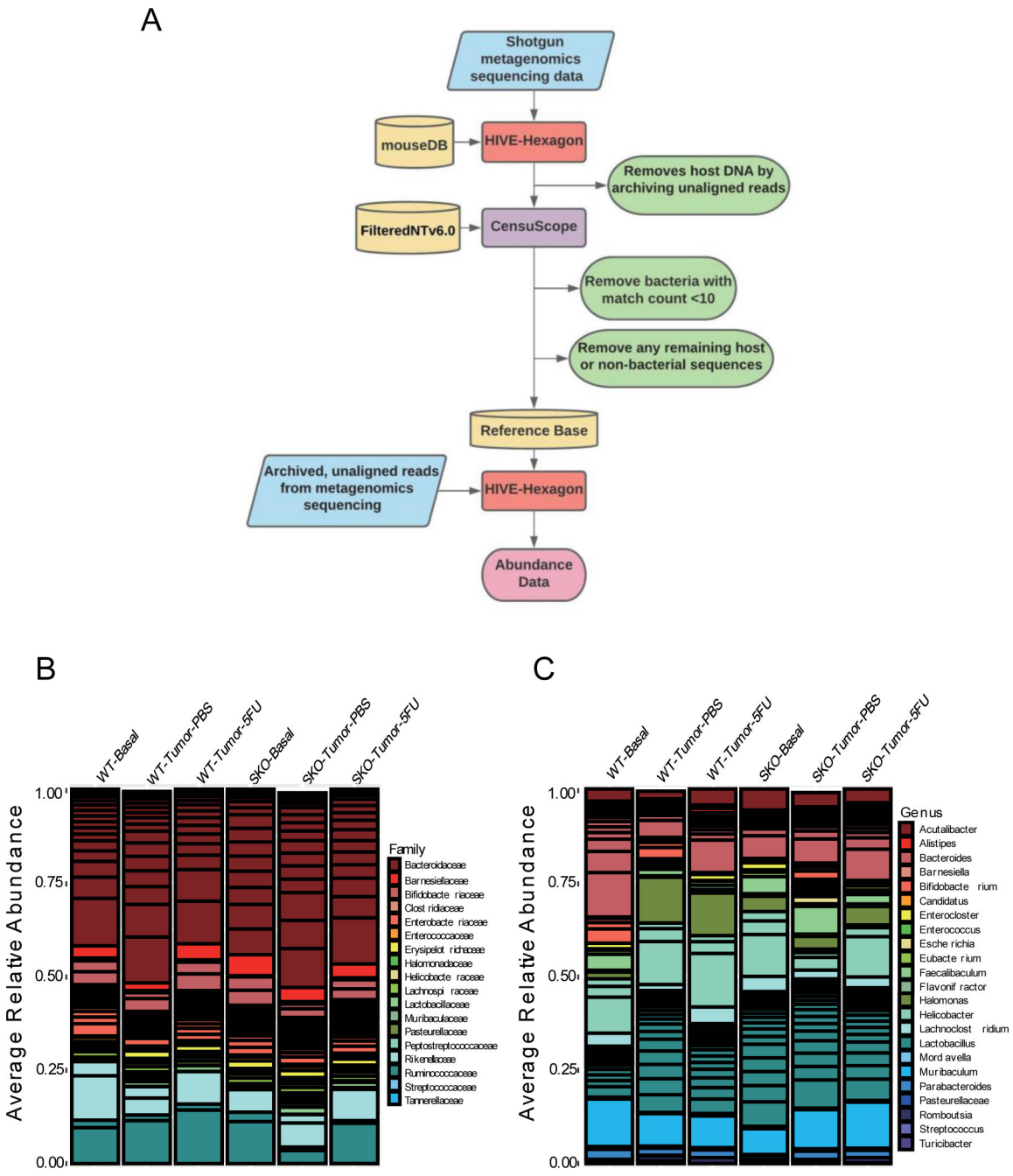

Figure 6.

Shotgun metagenomic sequencing data analyses of the gut microbiome. A) The bioinformatics analysis workflow utilizes two HIVE platform tools, CensuScope and HIVE-Hexagon. CensuScope is used to determine the taxonomic composition of each sample. HIVE-Hexagon is an alignment tool used to remove host DNA and determine the number of alignments or 'hits' made to the reference base. After the two-step metagenomics pipeline, relative abundance is calculated using the number of hits. The final abundance profile lists all the bacteria present in the samples and their relative abundances. B-C) Differences in gut microbiota composition on a family-level (B) and a genus-level (C) are observed in

mice fecal samples. The bar plots were generated using the Microbiome R package (https://microbiome.github.io/tutorials/). WT-basal, n = 16; WT-tumor-PBS, n = 7; WT-tumor-5FU, n = 7; SKO-PBS n = 8 (n = 5, *Smad4+/−Sptbn1+/−;* n = 3, *Smad4+/−*); SKO-5FU, n = 10 (n = 7, *Smad4+/−Sptbn1+/−;* n = 3, *Smad4+/−*).

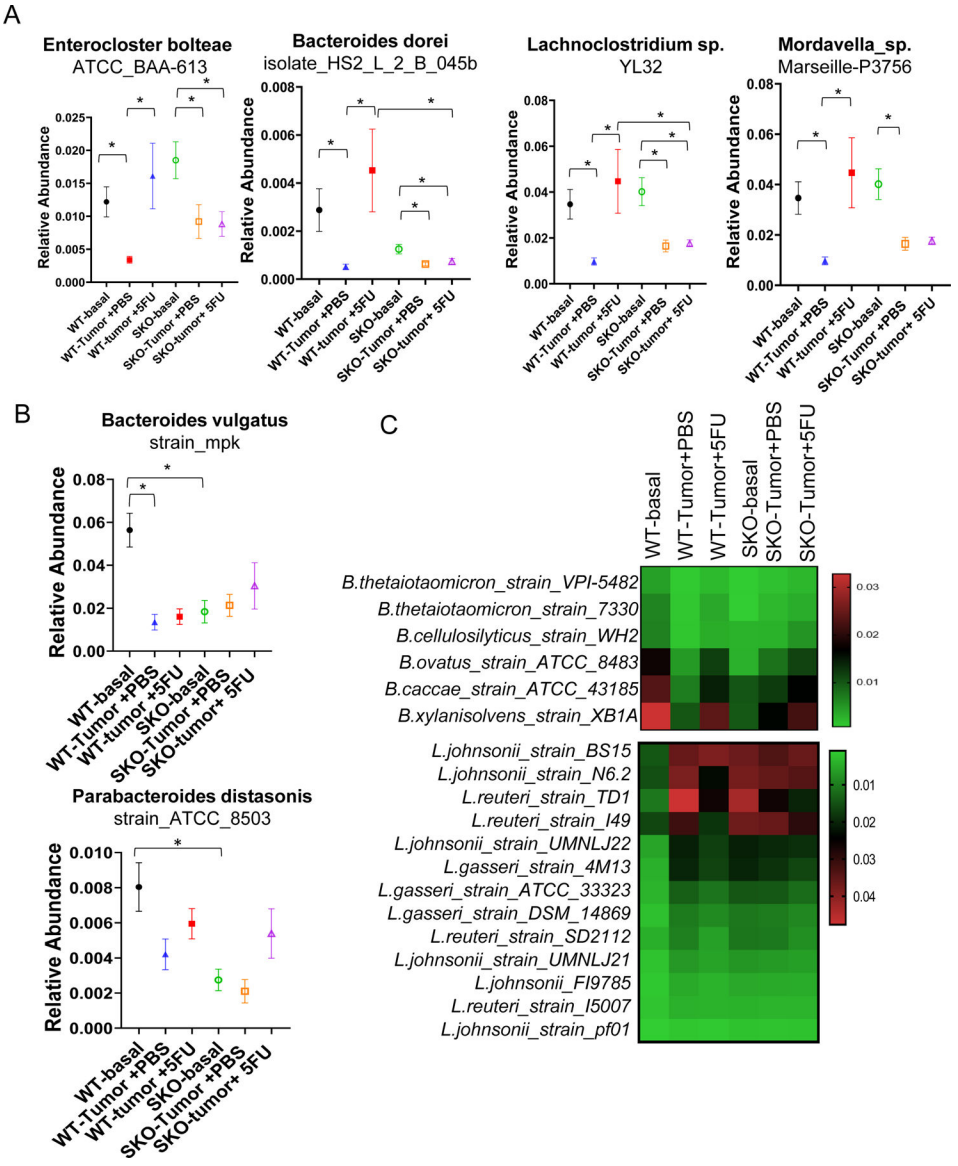

Figure 7.

Unique gut microbiome signature in 5FU resistant SKO, *Smad4+/–* and *Smad4+/–/Sptbn1+/–* CRCs. (A) Bacteria species and strains that are significantly reduced in AOM/DSS-induced tumors and recover to basal levels after 5FU treatment in WT mice but not in SKO mice. (B) Bacteria species and strains that are significantly reduced in AOM/DSS-induced tumors and SKO mice at basal levels before any treatment. Data in A-B are plotted as the average of relative abundance ± SEM, the significance is performed using an unpaired t-test, WT-basal, n = 16; WT-tumor + PBS, n = 7; WT-tumor + 5FU, n = 7; SKO-PBS, n = 16; SKO-tumor + PBS, n = 8 (n = 5, *Smad4+/−Sptbn1+/−;* n = 3, *Smad4+/−*); SKO-tumor + 5FU, n = 10 (n = 7, *Smad4+/−Sptbn1+/−;* n = 3, *Smad4+/−*); *p < 0.05. (C) A Heatmap of Bacteroides and Lactobacillus species and strains that are altered in AOM/DSS induced tumors and recovered to basal levels after 5FU treatment in WT mice but not recovered in SKO mice deficient in TGF-β signaling.

Table 1

Experiment mice number, tumor incidence, tumor number and size. SKO-PBS, *Smad4*$^{+/-}$*Sptbnb1*$^{+/-}$ (n = 5) and *Smad4*$^{+/-}$ (n = 3); SKO-5FU, *Smad4*$^{+/-}$*Sptbnb1*$^{+/-}$ (n = 7) and *Smad4*$^{+/-}$ (n = 3). Significance was determined using an unpaired t-test.

Group	Tumor incidence	Number of. tumors per animal (mean ± SE)	Average tumor size in mm (mean ± SE)
WT-PBS	6/8 (75%)	5.5±1.4	2.17±0.3
WT-5FU	4/8 (50%)	1.67±0.6[a]	0.83±0.3[a]
SKO-PBS	8/8 (100%)	10.25±1.5	3.63±0.7
SKO-5FU	10/10 (100%)	6.9±1.2[b]	2.5±0.3[b]

[a] $P < 0.05$, WT-PBS compared to WT-5FU

[b] $P > 0.1$, no significant difference between SKO-PBS and SKO-5FU

Table 2.

Histopathology of CRC tumors in WT and TGF-β signaling-deficient mice receiving PBS. SKO, *Smad4*$^{+/-}$*Sptbnb1*$^{+/-}$ (n = 5) and *Smad4*$^{+/-}$ (n = 3); WT (n = 6). Significance was determined using Chi-square test.

Group	Intraepithelial neoplasia Low-grade	Intraepithelial neoplasia high-grade	Adenocarcinoma	P value
WT-PBS	43%	38%	19%	0.003
SKO-PBS	17%	53%	30%	

Table 3.

Tumor size distribution. WT-PBS (n = 6); WT-5FU (n = 4); SKO-PBS, *Smad4*$^{+/-}$*Sptbnb1*$^{+/-}$ (n = 5) and *Smad4*$^{+/-}$ (n = 3); SKO-5FU, *Smad4*$^{+/-}$*Sptbnb1*$^{+/-}$ (n = 7) and *Smad4*$^{+/-}$ (n = 3). Significance was determined using Fisher's exact test.

Group	Tumor < 2 mm	Tumor 2 – 3 mm	Tumor > 2 mm
WT-PBS	16.7%	83.3%	0
WT-5FU[a]	83.3%	16.7%	0
SKO-PBS	0	37.5%	62.5%
SKO-5FU[b]	10%	80%	10%

[a] P = 0.02, WT-PBS compared to WT-5FU

[b] P = 0.11, no significant difference between SKO-PBS and SKO-5FU